WHAT MAKES SOME VENUSIAN CORONAE SO STEALTHY? L. Sabbeth[1], M. Carrington[2], and S. Smrekar[1], [1]Jet Propulsion Laboratory/California Institute of Technology, Pasadena, CA 91024 (leah.sabbeth@jpl.nasa.gov), [2]Department of Geological Sciences, Jackson School of Geosciences, The University of Texas at Austin, Austin, TX 78712.

Introduction: Coronae are circular to oblong features on the surface of Venus, ranging from 75 km to over 1000 km in diameter, identified by their circumferential set of fractures, or fracture annuli. They often have circumferential topographic rims and/or trenches, which do not necessarily correlate to fracture patterns. Classification systems exist based on fracture and topographic patterns: there are 5 classes of fracture annulus morphologies (concentric, concentric-double ring, radial/concentric, asymmetric, and multiple) [1] and 9 groups of topographic profile patterns, based on interior lows or highs and exterior troughs and/or rims [2]. Two types of coronae exist: regular coronae, or Type 1, which have ≥ 180° of a fracture annulus, and stealth coronae, or Type 2, which have < 180° of a fracture annulus [3].

Several formation mechanisms have been proposed for coronae, including mantle upwelling [4], coupled mantle upwelling and lithospheric dripping [2], lithospheric instabilities [5]–[7], and lithospheric subduction [8], [9]. Rims are typically modelled as a collapsing dome, with trenches due to dripping or subduction. Models generally predict specific patterns in topography or fracture placement, such that fractures should largely migrate outward, following the migration of maximum curvature of the topographic rims, with the exception of the case of subduction, where older fractures become subducted. More recent work suggests that topographic rims form above regions of upwelling and melt formation, rather than over a collapsing dome [9]

Stealth coronae background: Stealth coronae tend to be smaller, more commonly isolated, and found in plains than regular coronae [3]. All 9 groups of topographic forms are found in stealth coronae, indicating that their evolutionary stages cover a broad range [3]. Flexure studies show that elastic thicknesses at coronae are generally thin (mostly 5-15 km) [10], [11], but no significant difference has been reported in elastic thicknesses of stealth versus regular coronae [12]. Wider, larger plumes produce more complex topography, including depressions, and also coronae that are offset coronae from the plume center [13]. Laboratory experiments predict formation of asymmetric, arcuate trenches during subduction, which are observed in gravity data at coronae [14].

Several factors have been proposed to cause topographic rims coincident with missing fractures, including (1) a strong lithosphere, in which rims without fractures have less curvature, (2) slow viscous bending, which could allow rims for form without forming fractures, and (3) regional stress fields may suppress particular orientations of fractures [3]. Density and strain rate differences may cause these rim-only areas [15]. No comprehensive study yet quantifies circumferential variations in fracture annuli and topographic rims of stealth corona compared to regular coronae. We investigate differences between types 1 and 2 coronae, and begin by addressing quantitative differences in their fracture annuli and topographic patterns.

Methods: We map fracture annuli using Magellan SAR imagery, and produce 12 radial topographic profiles for 60 regular coronae, covered by stereo topography data from Magellan [16], and 40 stealth coronae, covered by Magellan altimetry. Using the radial profiles, we visualize fracture placement versus topographic rims, and quantify heights of topographic rims, widths of fracture annuli and rims, and radii of coronae (Figure 1). We use 9 groups to classify fracture placement relative to topographic rims (Figure 2), and classify each corona by the dominant group of its 12 radii.

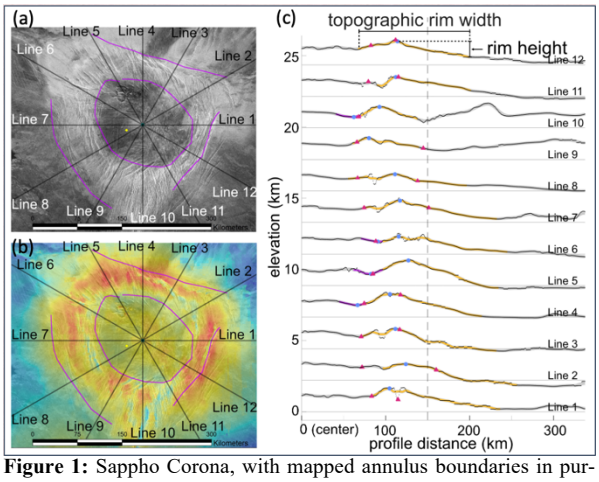

Figure 1: Sappho Corona, with mapped annulus boundaries in purple on SAR (a) and stereo-derived topography (Herrick et al., 2012) (b), and corresponding topographic profiles (c).

Preliminary results: Initial investigation shows that complexity exists in the continuity of fracture annuli stealth vs regular: even if a fracture annulus extends ≥ 180°, it may appear in several fragments rather than be continuous. Topographic rims are similarly complex: they do not necessarily extend ≥ 180° around coronae, nor do they necessarily overlap with fracture annuli.

More than half of all coronae radii have both topographic rims and fracture annuli. No coronae have a majority of profiles with the fractures fully interior to the topographic rims, and most coronae have fractures fully overlapping the rims (Figure 2).

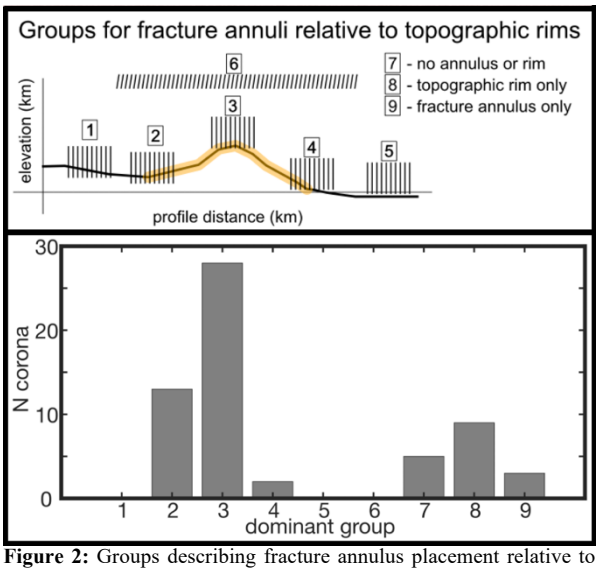

Figure 2: Groups describing fracture annulus placement relative to topographic rim (top) and fracture placement results for regular coronae (bottom).

Interpretations:

We expect fracture annuli to form at the point of maximum curvature on topographic rims, so the lack of fracture annuli fully interior to the topographic rims indicates that rims do not migrate far outward during corona evolution. It is possible that some inner fractures have been flooded with lava and are no longer visible.

Overall, we find that relationships between fracture annuli and topographic rims vary within individual coronae, circumferentially, as well as within the population of coronae. The distinction between regular coronae and stealth coronae is useful in depicting two endmembers of fracture annulus fullness, but does not address the complexity we see in regular or stealth coronae. From our initial work, we see the necessity to better characterize the placement of fracture annuli and topographic rims at coronae, and use this grouping to begin quantifying these characteristics.

Regional stresses are one plausible source of circumferential diversity in coronae – many coronae are proximal to rift zones, volcanoes, and other coronae. We begin to consider relationships between coronae and regional stresses. We continue our work also by quantifying topographic rims, heights, and fracture annulus widths, to determine whether these have any relation to the presence/overlap of fractures and topography.

Acknowledgments: A portion of this research was conducted at the Jet Propulsion Laboratory, California Institute of Technology, under contract with NASA.

References:

[1] E. R. Stofan *et al.* (1992) *JGR,* 97, 13347–13378.
[2] S. E. Smrekar and E. R. Stofan. (1997) *Science*, 277, 1289–1294.
[3] E. R. Stofan *et al.* (2001) *GRL,* 28, 4267–4270.
[4] D. M. Janes *et al.* (1992) *JGRP*, 97, 16055–16067.
[5] P. M. Grindrod and T. Hoogenboom. (2006) *Astronomy & Geophysics*, 47, 3–16.
[6] T. Hoogenboom and G. A. Houseman. (2006) *Icarus*, 180, 292–307.
[7] D. Piskorz, *et al.* (2014) *JGRP*, 119, 2568–2582.
[8] D. T. Sandwell and G. Schubert. (1992) *Science*, 257, 766–770.
[9] J. Schools and S. E. Smrekar. (2022) *LPSC LIV,* Abstract #1771.
[10] J. G. O'Rourke and S. E. Smrekar. (2018) *JGRP,* 123, 369–389.
[11] S. E. Smrekar, *et al.* (2022) *Nature Geoscience*, 1–6.
[12] A. Jiménez-Díaz, *et al.* (2015) *Icarus*, 260, 215–231.
[13] T. V. Gerya. (2014) *EPSL*, 391, 183–192.
[14] A. Davaille, *et al.* (2017) *Nature Geoscience*, 10, 349–355.
[15] S. E. Smrekar and E. R. Stofan. (2003) *JGRP*, 108.
[16] R. R. Herrick, *et al.* (2012) *Eos, Transactions AGU*, 93, 125–126.